Genesis of Typhoon Hagupit (2008) as revealed by ERA5 reanalyses and satellite observations

Minhee Chang[a] and Roger K. Smith[b]*
[a]*School of Earth and Environmental Sciences, Seoul National University, Seoul, South Korea*
[b] *Meteorological Institute, Ludwig-Maximilians University, Munich, Germany*
*Correspondence to: Prof. Roger Smith, Meteorological Institute, Ludwig-Maximilians University, Munich, Germany.
E-mail: roger.smith@lmu.de

Based on emerging ideas concerning the dynamics of tropical cyclogenesis and intensification, we hypothesize that an important distinguishing factor in determining whether or not an incipient tropical low disturbance will intensify to become a tropical storm is whether or not sustained deep convection develops at or close to the centre of circulation of the low. A feasibility study is presented for testing this hypothesis using satellite observations in conjunction with ERA5 reanalyses in the context of northwest Pacific typhoons. The satellite observations comprise the ocean wind vectors obtained from the Quick Scatterometer (QuikSCAT) and the brightness temperatures of infrared and water vapour channels obtained from the geostationary Multifunctional Transport Satellite-1R (MTSAT-1R). This pilot case study relates to the genesis of Typhoon Hagupit (2008) and the results suggest that the ERA5 reanalyses have sufficient fidelity for testing the foregoing hypothesis and that, indeed, the hypothesis is supported in this case.

Key Words: Tropical cyclones; typhoons; tropical genesis

Received July 3, 2021; Revised ; Accepted

Citation: . . .

1. Introduction

It is well established that tropical cyclones originate mainly from deep convective clusters over the warm tropical oceans. These are regions where conventional meteorological data are sparse and the interpretation of satellite imagery has an important role in forecasting genesis. The fact that only a small fraction of cloud clusters develop into tropical cyclones is a particular challenge to forecasters in determining which clusters will spawn a cyclone.

Considerable basic understanding of tropical cyclogenesis has emerged from field experiments such as the Tropical EXperiment in MEXico experiment (TEXMEX, Emanuel, ref), the Tropical Cyclone Structure 2008 experiment (TCS08, Elsberry and Harr 2008) and the Pre-Depression Investigation of Cloud Systems in the Tropics experiment (PREDICT, Montgomery et al. 2012) as well as from numerical modelling studies motivated by analyses of data collected during these experiments (e.g. Montgomery et al. 2010, Raymond and Carillo 2011, Smith and Montgomery 2012b, Smith and Montgomery 2012a, Davis and Ahijevych 2012, Wang 2012, 2014, Nicholls and Montgomery 2013, Lussier 2014, Davis 2015, Freismuth et al. 2016, Kilroy et al. 2017b,a, 2018).

The PREDICT experiment, in particular, was designed to test three main scientific hypotheses developed a few years earlier by Dunkerton et al. (2009) and supported by the results of cloud-representing idealized and real-scale numerical simulations by Montgomery et al. (2010) and Wang et al. (2010). The three hypotheses comprise an overarching framework for exploring synoptic, sub-synoptic, mesoscale and cloud-scale linkages in the formation of a tropical depression* vortex from a small, but

*The glossary on the NOAA Hurricane Research Division website uses "tropical cyclone" as "the generic term for a non-frontal synoptic-scale low-pressure system over tropical or subtropical waters with organized

finite amplitude, neutral or unstable easterly wave precursor disturbance. This framework is charmingly referred to as the "marsupial paradigm". The paradigm highlights in particular a favoured location, or sweet spot, for upscale vorticity growth and vorticity aggregation as well as the importance of a sub-synoptic-scale quasi-closed recirculating region, the so-called pouch, that acts to contain the moisture produced deep cumulus convection, helping to protect the incipient disturbance from the hostile environmental effects of dry air intrusion and vertical wind shear. One outcome of the PREDICT experiment was to verify these hypotheses (Montgomery et al. 2012).

Most studies of tropical cyclogenesis over other ocean basins have had to rely largely on remote sensing. One such study is that of Chang et al. (2017), who carried out a climatological study of deep convective cloud clusters over the northwest Pacific Ocean based on satellite observations and reanalyses, the aim being to investigate differences between clusters that underwent cyclogenesis and those which did not. A prominent feature of most clusters examined was the large diurnal variation in the areal extent of deep convection, an attribute that has been recognized for many years[†] (e.g. Gray and Jacobson 1977, Yang and Slingo 2001 and refs.).

Chang et al. (2017) quantified the diurnal increase in the area of deep convection from its afternoon minimum to morning maximum as well as the daily maximum areal extent of deep convection. In their study, deep convection was identified by a method explored by Olander and Velden (2009), which is based on the difference between two brightness temperature channels, a water vapour channel (6.5-7.0 μm) and an infra-red channel (10.3-11.3 μm). As noted by Schmetz et al. (1997), when convection penetrates the tropopause, water vapour has a higher brightness temperature than the infra-red cloud top temperature near the tropopause on account of the strongly reduced of atmospheric lapse rate in the stratosphere. Using the difference between the two brightness temperature enables one to distinguish active convective cells from the large area of cirrus cloud produced by the convection.

Chang et al. found that the area of deep convection, defined as the number 4 km $\times$ 4 km pixels where the brightness temperature difference was positive, fluctuates on the meso-β scale, the diurnal increase being larger than 5,000 km^2 and the daily maximum larger than 15,000 km^2 in most of the disturbances that developed (54 out of 80 cases), but also in several of those that did not (53 out of 383 cases). For those developing and non-developing disturbances having a comparable area of deep convection, the composite analysis of relative vorticity from the reanalysis showed that the areal averaged vertiical vorticity within 500 km radius of the vorticity maximum at the beginning of the first fluctuation was similar also between the two disturbance groups. Significantly, the areal averaged vertical wind shear in the annular region from 300 km to 800 km radius around the location of the vorticity maximum was markedly stronger for non-developing disturbances than for developing disturbances, which may explain why these failed to develop.

Whether or not a particular cloud cluster develops into a tropical cyclone must depend, in part, on the location of the deep convective updraughts in relation to the centre of the incipient cyclonic circulation in which the convection is embedded. This is because the location of deep convection close to this centre is geometrically most favourable for the overturning circulation induced by the convection to converge cyclonic vertical vorticity towards the centre of the incipient circulation (Smith and Montgomery 2016, Kilroy and Smith 2016). When located off the axis, deep convection will induce a low-level flow on its side nearest the centre that is radially outward. The foregoing ideas are supported by statistical analyses of airborne Doppler radar observations of Atlantic hurricanes by Rogers et al. (2013), who found that in rapidly intensifying storms, there is a tendency for vigorous deep convective bursts to occur inside the radius of maximum tangential winds. This preferred location of deep convection close to this centre explains also why in idealized numerical simulations starting with initial vortices with same intensity, but different radial size, the gestation period leading up to genesis increases with radial size. It turns out that the smaller the initial vortex size, boundary layer convegence focusses early convection closer to the axis of circulation (Kilroy and Smith 2017).

Similar considerations to those above would appear relevant to explaining why some cloud clusters in the tropics develop into tropical cyclones, while others do not. In order to explore this idea based on observations, it would be necessary to be able to determine the centre location of an incipient cloud cluster circulation with sufficient accuracy. It is the purpose of the present paper to explore the feasibility of such a determination using a well-documented case of tropical cyclogenesis as an example.

The recent release of the ERA5 global reanalysis data (Hersbach and Coauthors 2020) provides an opportunity to examine the circulation associated with observed cloud clusters with unprecedented spatial and temporal resolution (see below for details) and they have the potential for obtaining sufficiently accurate centre locations for the study proposed above. In a recent paper, Hodges et al. (2017) examined how well tropical cyclones are captured in various reanalysis data sets, but their review did not consider the formation stage of tropical cyclones. In this study, we investigate the possible accuracy with which a pre-tropical cyclone disturbance in satellite observations can be captured by the ERA5 reanalyses and go on to investigate the process of genesis in these data. Under satellite observations, we include the surface wind fields derived from data obtained by the polar orbiting satellite, QuikScat, which provide a possibility to determine the centre locations of tropical disturbances at the surface, albeit at asynoptic times.

2. Data and Methodology

The focus of this study is the case of Typhoon pre-Hagupit (2008) during the period 12 UTC on 17 September to

convection (i.e. thunderstorm activity) and a definite cyclonic surface wind circulation". Notably, this definition does not invoke any wind threshold. The same glossary defines a "tropical depression" as "a tropical cyclone with maximum sustained surface winds of less than 17 m s^{-1} (34 kt, 39 mph) and, in the Atlantic and Eastern Pacific Basins, a tropical storm as a tropical cyclone with surface winds between 17 and 33 m s^{-1}. Essentially the same definitions are used by the Joint Typhoon Warning Center for the North Pacific Ocean, except the term "typhoon" is used instead of "hurricane". In this study we follow the designations in the JTWC best-track data.

[†]Typically, tropical oceanic deep convection has a strong diurnal signal different from that over land with cirrus cover and rainfall having a peak in the early morning hours

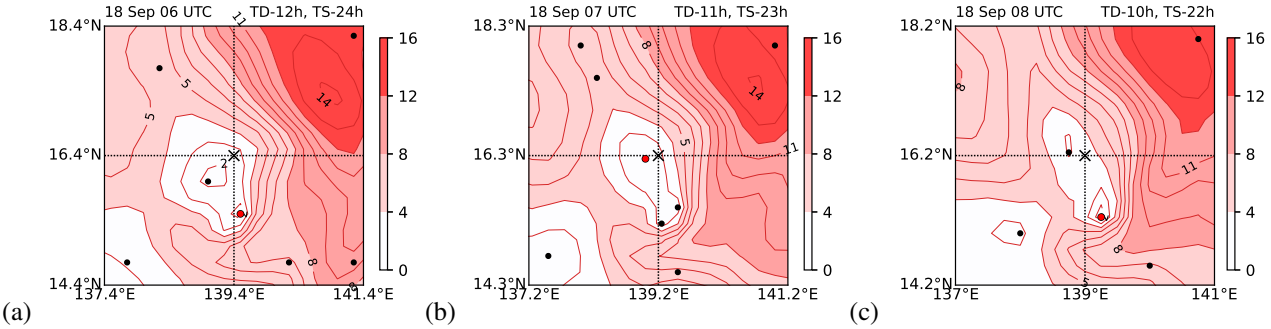

Figure 1. Horizontal winds (m s^{-1}; shading and vectors) at 1000 hPa around pre-Hagupit at (a) 06 UTC, (b) 07 UTC, and (c) 08 UTC on 18 September. The information at top right of each panel indicates the relative time (h) before tropical depression (TD) or tropical storm (TS) formation. The centre of the domain (black crosses) corresponds to the centre location of pre-Hagupit in the JTWC best track. Black dots indicate the location of local wind speed minima and the red dots indicate the location of the absolute minimum.

00 UTC 20 September. This typhoon occurred during the Tropical Cyclone Structure 2008 (TCS08) field experiment and was the focus of an earlier study based on airborne Doppler radar observations by Bell and Montgomery (2010). The foregoing analysis period corresponds with 42 h before to 18 h after the storm was designated as a tropical storm (1-minute sustained wind speed $\geq$ 34 knots) by the Joint Typhoon Warning Center (JTWC) best track data. During the analysis period, pre-tropical storm and tropical storm locations are obtained from JTWC best track at 6 hr intervals. The storm locations are linearly interpolated to 1 hr intervals for use as first guess when determining the location of near-surface minimum wind speed or geopotential height from the reanalysis data.

2.1. ERA5 Reanalysis data

The global reanalysis data, ERA5, are available at 1 hr intervals on a $0.25^o \times 0.25^o$ longitude-latitude grid. To examine how well tropical cyclone formation is captured in the reanalysis, geopotential height, zonal and meridional wind speed, vertical velocity and the vertical component of relative vorticity at the surface and at 1000, 900, 700 and 500 hPa around a pre-tropical cyclone are analyzed.

2.2. Satellite data

The observations from two satellites are used as a reference to validate the reanalysis data.

First, the Quick Scatterometer (QuikSCAT) Level 2B Ocean Wind Vectors of Version 4.1 are used to examine the surface winds. The polar orbiting satellite QuikSCAT made passes over pre-Typhoon pre-Hagupit three times during the analysis period: at 21 UTC 17 September, 9 UTC 18 September and 22 UTC 19 September. At those times, surface wind speed and direction are obtained on a 25 $\times$ 25 km grid. The effects of rain contamination on the observed wind speed are corrected using neural network techniques and the mean absolute error of corrected wind speed is about 3 m/s (Stiles and Dunbar 2010, Stiles et al. 2014).

Second, the geostationary Multifunctional Transport Satellite-1R (MTSAT-1R) data are used to determine the location of deep convection. These data are available at 1 hr intervals with 4 km pixel resolution. The brightness temperatures in the infrared channel (IR; centred at 10.8 μm) and water vapour channel (WV, centred at 6.75 μm) are obtained. The location of deep convection is determined by taking the difference between two brightness temperatures (IR minus WV) using the algorithm employed by Olander and Velden (2009).

3. Results

3.1. Centre finding procedure

As a first step to comparing how well a pre-tropical cyclone disturbance in satellite observations is captured by the ERA5 re-analysis data, it is necessary to determine the centre location of the proto-vortex circulation in the re-analysis data and compare this location, where possible, with that in the QuikSCAT data. There are, of course, several ways to define the "centre location" of the vortex in the analyses. Possible choices would be the location of the minimum horizontal wind speed or the minimum geopotential height on some pressure level. Here we use the location of these minima at 1000-hPa, 900-hPa and 700-hPa. As a first guess, we use the position of the disturbance centre in the JTWC best track data at the relevant time. Then, a search is carried out for the various mimima within a 2-degree latitude $\times$ 2-degree longitude box.

As exemplified by Figure 1, there may exist more than one local minimum in the search domain at a given time. These local minima are shown as the black dots in the figure. Among the multiple minima, a centre can be defined in various ways, such as choosing an absolute minimum, the one closest to the JTWC best track, or the one closest to the previous or later time step. In this study, a centre is defined as a location of the absolute minimum of the particular quantity, recognizing the need for real time applicability of the method by operational centres. With this definition, the centre location can jump around as local centres appear and disappear, especially while the nascent circulation is still weak. Such behaviour is seen in the 1 hr snapshots in Figure 1. Nevertheless, this behaviour is to be expected on physical grounds since local circulations are associated with transient convective systems whose growth and decay has a stochastic element.

Using the same methodology, a search is carried out for the location of the minimum wind speed at reference height of 10 m from the QuikSCAT data at the three times when these data are available.

The tracks of the various centre locations are shown in Figure 2 and the mean differences in these locations are

Table I. Average distance (km) between the vortex centres at each time along the tracks shown in Fig. 2. The tracks are those of the location of minimum wind speed (Wind; red) and minimum geopotential height (GPH; blue) and at 1000-hPa, 900-hPa and 700-hPa from ERA5, location of minimum wind speed from QuikSCAT observation and JTWC best track of pre-Hagupit from 12 UTC on 17 September to 00 UTC 20 September. Distance from QuikSCAT is an average of three available time steps (shown in Fig. 2) and that from JTWC best track (black) is an average of the entire period in 6 hr intervals.

	1000 hPa		900 hPa		700 hPa		
	WND	GPH	WND	GPH	WND	GPH	JTWC
QuikSCAT	76	90	72	78	128	76	57
JTWC	82	67	83	62	123	92	
	78		59		78		

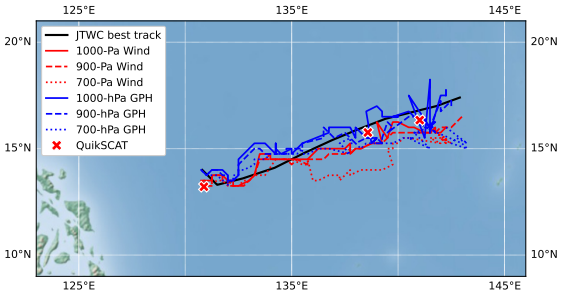

Figure 2. JTWC best track (black), track of the location of minimum wind speed (Wind; red) and minimum geopotential height (GPH; blue) at 1000-hPa (solid), 900-hPa (dashed) and 700-hPa (dotted) from ERA5, and minimum location of wind speed from QuikSCAT observation (red crosses) of pre-Hagupit from 12 UTC on 17 September to 00 UTC 20 September.

summarized in Table I. From the table it is seen that, on average, the JTWC best track location is closest to the centre location from QuikSCAT (average difference 57 km), while the metric from the ERA5 analysis that is closest to QuikSCAT on average is the location of the minimum wind speed at 900 hPa (average difference 72 km) with that of the minimum wind speed at 1000 hPa being next closest (average difference 76 km). The larger differences between the two metrics at 700 hPa are presumably a reflection of the existence of some degree of ambient vertical wind shear.

The average location difference between the minimum wind speed and minimum geopotential in the ERA5 reanalysis is 78 km at 1000 hPa, 59 km at 900 hPa and 78 km at 700 hPa. On average, the ERA5 900 hPa geopotential minimum is closest to the JTWC best track positions (average distance 62 km) with that of 1000 hPa geopotential minimum being next closest (average distance 67 km). The locations of the minimum wind speed at 900 hPa are the closest to location of minimum wind speed from the QuikSCAT observation and are chosen to define the disturbance centre in this study.

In summary, the foregoing analysis points to an intrinsic fuzziness in determining a representative centre position at a particular location at any given time. This fuzziness was anticipated, but needed to be quantified to pursue the aims of the paper, which are focussed on the hypothesized need to have sustained convection near the centre of an existing circulation to support tropical cyclone formation. Except at times of QuikSAT passages, the ERA5 analyses are the only data available to estimate centre locations of the precursor disturbance of the typhoon.

3.2. Near-surface wind distribution

Figure 4 compares the surface (10 m) wind vectors from the ERA5 reanalyses with ocean wind vectors observed during two QuikSCAT overpasses. The time difference between the overpasses and the analyses are within 30 minutes in each case. At 21 UTC 17 September (Figure 4a), the surface wind distribution in ERA5 shows a clear cyclonic circulation, with the strongest wind speeds located to the north of the disturbance centre in the annulus between the two circles of radius 1 and 5 deg. and the weakest wind speeds located to the southwest of the centre in the annulus between radii 3 and 5 deg.

The wind distribution in QuikSCAT near this time (Figure 4b) shows a clear cyclonic circulation also with the location of minimum wind speed displaced about 0.76 degrees in latitude from that of ERA5. The QuikSCAT wind distribution is noisier than in ERA5 and has wind speeds larger than 14 m s^{-1} at several points. However, when excluding these outliers, the distribution shows the strongest winds to the north of the disturbance centre in the annular region between the two circles with radii 1 and 5 deg. and the lowest wind speeds to the southwest of the centre to the southwest in the annular region between the two circles with radii 3 and 5 deg.

At 09 UTC 18 September (Figure 4c), the surface wind distribution in ERA5 is similar to that at the previous time, including the regions of strongest and weakest wind speeds. The distribution in QuikSCAT is overall consistent with that at previous time also. The location of minimum wind speed of QuikSCAT is displaced about 0.84 degree in latitude from that of ERA5. This time, however, the regions of strongest and weakest winds are observed 3 deg. southwest and southeast of the disturbance centre, respectively, which are different from those in ERA5. A broader region of wind speeds larger than 10 m s^{-1} occurs to the north of the disturbance centre, similar to that in ERA5.

3.3. Marsupial pouch

As discussed in the Introduction, the marsupial paradigm hypothesizes that tropical cyclogenesis is favoured by the existence of a region of closed circulation in a frame of reference moving with the nascent vortex. For this reason, it is pertinent to enquire whether such a pouch region exists in the case of the pre-Hagupit disturbance and, if so, whether it persists. To this end we calculated the relative flow by subtracting the velocity of the pre-Hagupit disturbance centre from the horizontal wind vectors. The velocity of the pre-Hagupit disturbance is obtained by taking a centred difference between 1 hr centre locations based on the minimum wind speed at a particular pressure level. The

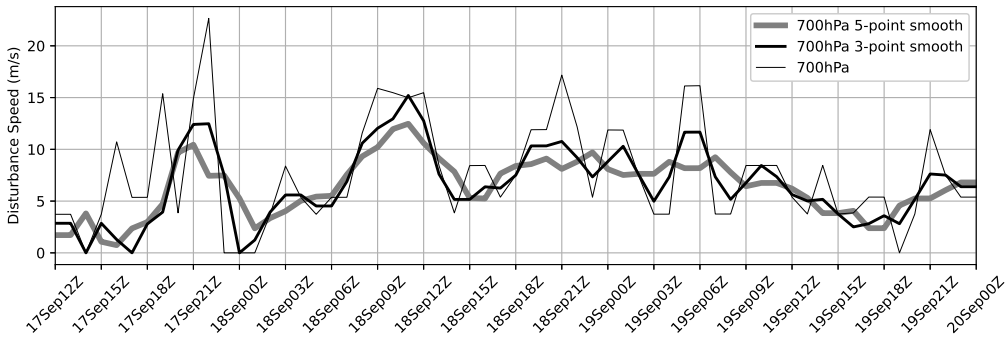

Figure 3. Time series of the centre speed of the low calculated as a centred-difference of the centre locations at 700 hPa. Thin curves are the raw speeds, intermediate thickness with 3-point smoothing, thickest curves 5-point smoothing.

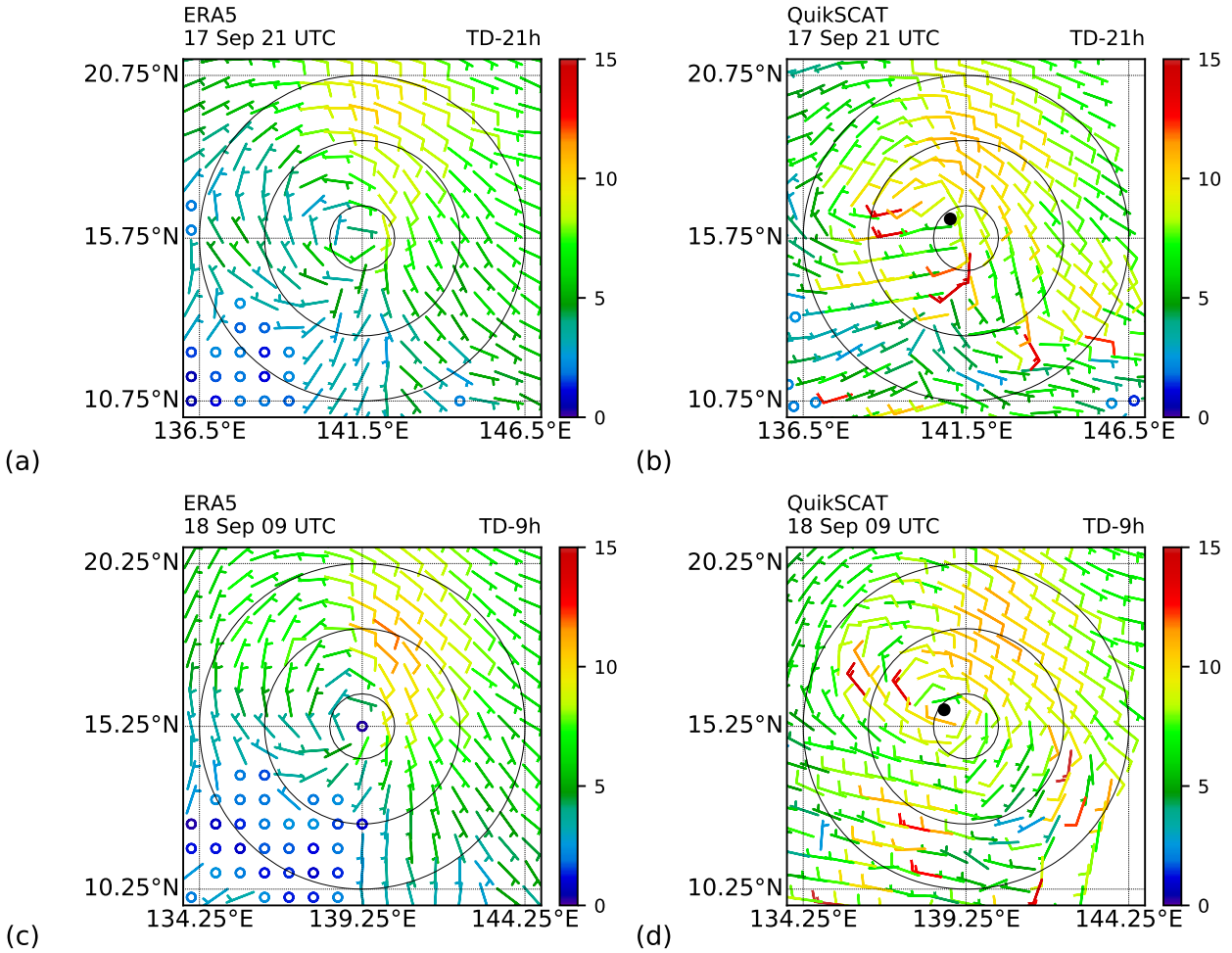

Figure 4. Horizontal wind barbs at the surface (nominally 10 m) obtained from ERA5 (left) and ocean wind barbs obtained from QuikSCAT (right) around pre-Hagupit at (a, b) 21 UTC on 17 September and (c, d) 09 UTC on 18 September. The information at top right of each panel indicates the relative time (h) before tropical depression (TD) formation. Each figure domain is centred at the location of minimum wind speed at 1000 hPa in ERA5, while black dot indicates the location of minimum wind speed of ocean wind vectors obtained from QuikSCAT. The radius of concentric circles are 1, 3 and 5-deg. around the red dot. Wind speeds less than 2.5 m s^{-1} are denoted by small circles.

speeds so obtained are shown in Figure 5 for the 700 mb pressure level. The raw speeds have occasional large spikes which are a result of the centre location jumping from one small area of weak wind speed to another within the central region of the broader-scale circulation. Using the raw speeds leads to dramatic changes in the relative streamlines over a large region. As seen in Figure 5, the large spikes can be substantially removed by applying mild smoothing to the centre locations. For the relative streamline calculations we applied a five-point smoothing operator to the centre locations.

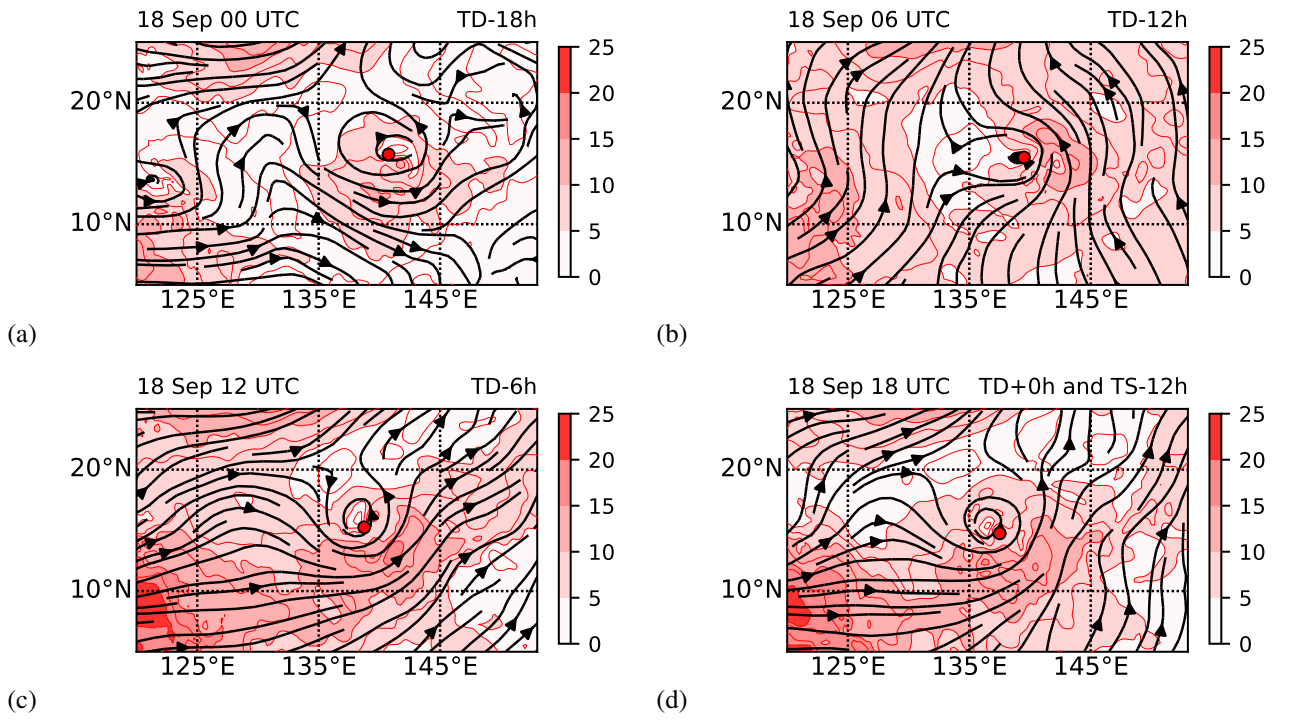

Figure 5. Relative streamlines (black curves) and relative horizontal wind speeds (m s^{-1}; shadings) at 700 hPa around pre-Hagupit at (a) 00 UTC, (b) 06 UTC, (c) 12 UTC, (d) 18 UTC on 18 September. The information at top right of each panel indicates the relative time (h) before tropical depression (TD) or tropical storm (TS) formation. The red dot indicates the centre of pre-Hagupit at 900 hPa.

Figure 5 shows the relative streamlines and isotachs of relative wind speed at 700 hPa at 6 hr intervals on the day leading up to the disturbance being deemed a tropical depression by JTWC (18 UTC 18 September). At all times, there is a saddle point in the streamlines located to the northwest or west of the disturbance centre that could allow the entry of environmental air into the broader circulation surrounding the disturbance, but by the time the disturbance was classified as a depression, an inner region of closed streamlines had formed to provide a protective pouch, 1-2 deg. in diameter, to support further intensification. Note that at all times, the disturbance centre, which refers to the minimum wind speed at 900 hPa as defined in Section 3.1, is relatively close (< 1 deg. latitude) to the centre of the closed gyre in the relative streamline at 700 hPa.

3.4. Evolution of deep convection

Figure 6 shows the location of deep convection in the pre-Hagupit disturbance as determined from the MTSAT-1R brightness temperature difference between the infrared and water vapour channels. It shows also isopleths of geopotential height at 900 hPa and selected contours of vertical velocity from the ERA5 analyses.

At 00 UTC 18 September (Figure 6a), the satellite imagery shows two convective complexes, one just to the west and a closer one to the southwest of the circulation centre at 900 hPa. The ERA5 analysis shows several deep convective cells overlapping with these systems as highlighted by the yellow contours of vertical velocity exceeding 0.1 m s^{-1}. One of these cells is located just to the southeast of the circulation centre. Six hours later (Figure 6b), one of the two observed systems has moved westwards and the other has moved southwestwards and their distance from the analysed disturbance centre has increased. However, the ERA5 analysis shows increased convection within the disturbance circulation with one cell just to the west of the centre. These analysed cells only partially overlap with the observed convective system to the southwest of the centre and there are no cells overlapping with the system to the west of the disturbance.

At 18 UTC 18 September (Figure 6c), 6 hr before the disturbance was declared a tropical depression by JTWC, the satellite imagery shows just one convective complex and this overlaps the analysed circulation centre. Moreover, the analysis captures an intense deep convective cell with an updraught exceeding 0.2 m s^{-1} overlapping with the observed convective system. At the time the disturbance was declared a tropical depression (18 UTC 18 September, Figure 6c), the observed convective system had expanded in area while retaining an overlap with the analysed circulation centre. Again, the analysed vertical motion showed several cells overlapping the observed convective system, one of them with an updraught exceeding 0.2 m s^{-1}.

3.5. Summary and implications

In summary, the ERA5 reanalyses have skill in locating the observed near-surface circulation in the case of pre-Typhoon Hagupit and show that by the time the storm was classified by JTWC as a tropical depression, it had already developed a protective pouch-like closed circulation in the lower troposphere. Further, analyses of satellite imagery highlighting locations of deep convection shows that deep convection was persistent near or at the circulation centre as the storm developed, a feature captured also by the ERA5 analysis. As discussed in the Introduction, from a theoretical viewpoint, this is an optimal location to promote vortex intensification. Our analyses provide confidence in using the ERA5 reanalyses together with satellite analyses

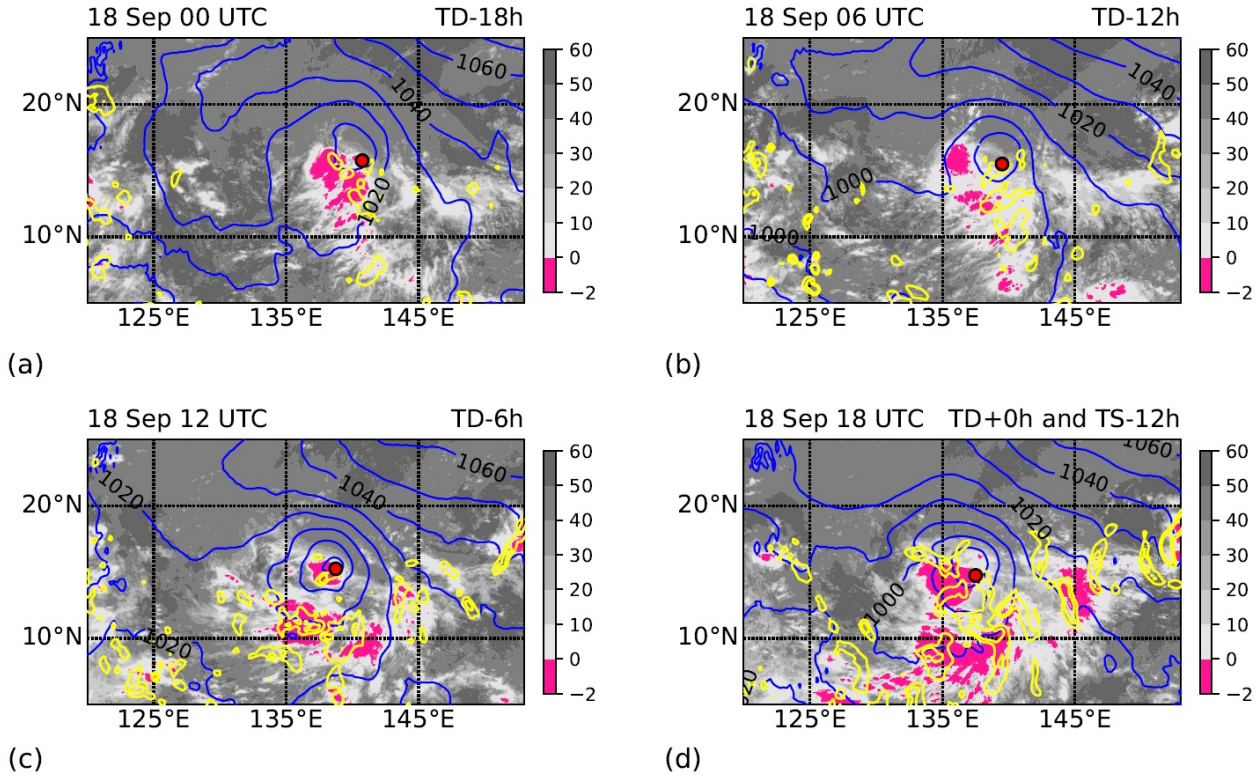

Figure 6. Geopotential height at 900 hPa (m; blue contours), vertical velocity at 500 hPa (0.1 and 0.2 m s^{-1}; yellow contours) and MTSAT-1R brightness temperature difference between the infrared and water vapour channels (K, shadings) around pre-Hagupit at (a) 00 UTC, (b) 06 UTC, (c) 12 UTC, (d) 18 UTC on 18 September. The information at top right of each panel indicates the relative time (h) before tropical depression (TD) or tropical storm (TS) formation. Red dot indicates a centre of pre-Hagupit.

of the type used here to address the hypothesis that an important distinguishing factor in determining whether or not an incipient tropical low disturbance will intensify to become a tropical storm is whether or not sustained deep convection develops at or close to the centre of circulation of the low. Further, the analyses for pre-Typhoon Hagupit are consistent, at least, with the foregoing analysis, although cases of non development have not been addressed in this study. A next step will be to carry out an extended analysis applied to multiple cloud clusters, both developing and non-developing clusters, during one or many typhoon seasons. This step will be required to refine the precise meaning of "close to the centre of circulation of the low" in the foregoing hypothesis. If successful, such a study might pave the way for improving the use of numerical forecast models to assess the likelihood of tropical cyclogenesis.

4. Conclusions

Using satellite observations in conjunction with ERA5 reanalyses, we have carried out a feasibility study for testing the hypothesis that an important distinguishing factor in determining whether or not an incipient tropical low disturbance will intensify to become a tropical storm is whether or not sustained deep convection develops close to the centre of circulation of the low. In a case study of the genesis of northwest Pacific Typhoon Hagupit in 2008, we used specialized analyses of satellite data to highlight locations of deep convection, ocean wind data from QuikSCAT, when available, to locate the centre of low-level circulation, and ERA5 analyses to estimate the centre location at other times as well as the broad-scale circulation patterns at these times. Our pilot study suggests that the reanalyses have sufficient fidelity for testing the foregoing hypothesis using multiple cases. Moreover, they show that the hypothesis is supported in the case of Typhoon Hagupit.

A test of the hypothesis using multiple cases is planned. If validated, the hypothesis could have utility in forecasting the likelihood of tropical cyclogenesis.

5. Acknowledgments

The first author acknowledges support from the Basic Science Research Program through the National Research Foundation of Korea (NRF) funded by the Ministry of Education (NRF2021R1I1A1A0105746711).

References

Bell, M. M. and M. T. Montgomery, 2010: Sheared deep vortical convection in predepression Hagupit during TCs08. *Geophys. Res. Lett.*, **37**, L06802.

Chang, M., C.-H. Ho, M.-S. Park, J. Kim, and M.-H. Ahn, 2017: Multiday evolution of convective bursts during western North Pacific tropical cyclone development and non development using geostationary satellite measurements. *J. Geophys. Res. Atmos.*, **122**, 1635–1649.

Davis, C. A., 2015: The formation of moist vortices and tropical cyclones in idealized simulations. *J. Atmos. Sci.*, **72**, 3499–3516.

Davis, C. A. and D. A. Ahijevych, 2012: Mesoscale structural evolution of three tropical weather systems observed during PREDICT. *J. Atmos. Sci.*, **69**, 1284–1305.

Dunkerton, T. J., M. T. Montgomery, and Z. Wang, 2009: Tropical cyclogenesis in a tropical wave critical layer: easterly waves. *Atmos. Chem. Phys.*, **9**, 5587–5646.

Elsberry, R. E. and P. Harr, 2008: Tropical cyclone structure (TCS08) field experiment scientific basis, observational platforms, and strategy. *Asia-Pacific J. Atmos. Sci.*, **44**, 1–23.

Freismuth, T. M., B. Rutherford, M. A. Boothe, and M. T. Montgomery, 2016: Why did the storm ex-gaston (2010) fail to redevelop during the (predict) experiment? *Atmos. Chem. Phys.*, **16**, 8511–8519.

Gray, W. M. and R. W. Jacobson, 1977: Diurnal variation of deep cumulus convection. *Mon. Wea. Rev.*, **105**, 1171–1188.

Hersbach, H. and Coauthors, 2020: The ERA5 global reanalysis. *Quart. J. Roy. Meteor. Soc.*, **147**, 1999–2049.

Hodges, K., A. Cobb, and P. L. Vidale, 2017: The ERA5 global reanalysis. *J. Clim.*, **30**, 5243–5264.

Kilroy, G., M. T. Montgomery, and R. K. Smith, 2017a: The role of boundary-layer friction on tropical cyclogenesis and subsequent intensification. *Quart. Journ. Roy. Meteor. Soc.*, **143**, 2524–2536.

Kilroy, G. and R. K. Smith, 2016: A numerical study of deep convection in tropical cyclones. *Quart. J. Roy. Meteor. Soc.*, **142**, 3138–3151.

— 2017: The effects of initial vortex size on hurricane genesis and intensification. *Quart. J. Roy. Meteor. Soc.*, **143**, 2832–2845.

Kilroy, G., R. K. Smith, and M. T. Montgomery, 2017b: A unified view of tropical cyclogenesis and intensification. *Quart. Journ. Roy. Meteor. Soc.*, **143**, 450–462.

— 2018: The role of heating and cooling associated with ice processes on tropical cyclogenesis and intensification. *Quart. Journ. Roy. Meteor. Soc.*, **144**, 99–114.

Lussier, L. L., 2014: The genesis of Typhoon Nuri as observed during the Tropical Cyclone Structure 2008 (TCS-08) field experiment - Part 3: Dynamics of low-level spin-up during the genesis. *Atmos. Chem. Phys.*, **14**, 8795–8812.

Montgomery, M. T., C. Davis, T. Dunkerton, Z. Wang, C. Velden, R. Torn, S. Majumdar, F. Zhang, R. K. Smith, L. Bosart, M. M. Bell, J. S. Haase, A. Heymsfield, J. Jensen, T. Campos, and M. A. Boothe, 2012: The pre-depression investigation of cloud systems in the tropics (predict) experiment: Scientific basis, new analysis tools, and some first results. *Bull. Amer. Meteor. Soc.*, **93**, 153–172.

Montgomery, M. T., Z. Wang, and T. J. Dunkerton, 2010: Coarse, intermediate and high resolution numerical simulations of the transition of a tropical wave critical layer to a tropical storm. *Atmos. Chem. Phys.*, **10**, 10803–10827.

Nicholls, M. and M. T. Montgomery, 2013: An examination of two pathways to tropical cyclogenesis occurring in idealized simulations with a cloud resolving numerical model. *Atmos. Chem. Phys.*, **13**, 5999–6022.

Olander, T. L. and C. S. Velden, 2009: Tropical cyclone convection and intensity analysis using differenced infrared and water vapor imagery. *Wea. Forecasting*, **24**, 1558–1572.

Raymond, D. J. and C. L. Carillo, 2011: The vorticity budget of developing Typhoon Nuri (2008). *Atmos. Chem. Phys.*, **11**, 147–163.

Rogers, R. F., P. D. Reasor, and S. Lorsolo, 2013: Airborne doppler observations of the inner-core structural differences between intensifying and steady-state tropical cyclones. *Mon. Wea. Rev.*, **141**, 2970–2991.

Schmetz, J., S. Tjemkes, M. Gube, and L. van de Berg, 1997: Monitoring deep convection and convective overshooting with meteosat. *Adv. Space Res.*, **19**, 433–441.

Smith, R. K. and M. T. Montgomery, 2012a: How important is the isothermal expansion effect to elevating equivalent potential temperature in the hurricane inner-core? *Quart. Journ. Roy. Meteor. Soc.*, **138**, 75–84.

— 2012b: Observations of the convective environment in developing and non-developing tropical disturbances. *Quart. Journ. Roy. Meteor. Soc.*, **138**, 1721–1739.

— 2016: The efficiency of diabatic heating and tropical cyclone intensification. *Quart. Journ. Roy. Meteor. Soc.*, **142**, 2081–2086.

Stiles, B. W., R. E. Danielson, W. L. Poulsen, S. Hristova-Veleva, Y.-P. Shen, and A. G. Fore, 2014: Optimized tropical cyclone winds from QuikSCAT: A neural network approach. *IEEE Transactions on Geoscience and Remote Sensing*, **52**, 7418–7434.

Stiles, B. W. and R. S. Dunbar, 2010: A neural network technique for improving the accuracy of scatterometer winds in rainy conditions. *IEEE Transactions on Geoscience and Remote Sensing*, **48**, 3114–3122.

Wang, Z., 2012: Thermodynamic aspects of tropical cyclone formation. *J. Atmos. Sci.*, **69**, 2433–2451.

— 2014: Role of cumulus congestus in tropical cyclone formation in a high-resolution numerical model simulation. *J. Atmos. Sci.*, **71**, 1681–1700.

Wang, Z., M. T. Montgomery, and T. J. Dunkerton, 2010: Genesis of pre-hurricane felix (2007). part i: The role of the easterly wave critical layer. *J. Atmos. Sci.*, **67**, 1711–1729.

Yang, G.-Y. and J. Slingo, 2001: The diurnal cycle in the tropics. *Mon. Wea. Rev.*, **129**, 784–801.